Neuro-Oncology 13(5):546–557, 2011.
doi:10.1093/neuonc/noq194
Advance Access publication February 4, 2011

Serial analysis of imaging parameters in patients with newly diagnosed glioblastoma multiforme

Yan Li, Janine M. Lupo, Mei-Yin Polley, Jason C. Crane, Wei Bian, Soonmee Cha, Susan Chang, and Sarah J. Nelson

Department of Radiology and Biomedical Imaging (Y.L., J.M.L., J.C.C., W.B., S.C., S.J.N.), Department of Neurological Surgery (M.-Y.P., S.C.), Department of Bioengineering and Therapeutic Sciences (S.J.N.), University of California, San Francisco

The objective of this study was to test the predictive value of serial MRI data in relation to clinical outcome for patients with glioblastoma multiforme (GBM). Sixty-four patients with newly diagnosed GBM underwent conventional MRI and diffusion-weighted and perfusion-weighted imaging postsurgery and prior to radiation/chemotherapy (pre-RT), immediately after RT (post-RT), and every 1–2 months thereafter until tumor progression, up to a maximum of 1 year. Tumor volumes and perfusion and diffusion parameters were calculated and subject to time-independent and time-dependent Cox proportional hazards models that were adjusted for age and MR scanner field strength. Larger volumes of the T2 hyperintensity lesion (T2ALL) and nonenhancing lesion (NEL) at pre-RT, as well as increased anatomic volumes at post-RT, were associated with worse overall survival (OS). Higher normalized cerebral blood volumes (nCBVs), normalized peak height (nPH) and normalized recirculation factors (nRF) at pre-RT, and nCBV at post-RT, in the T2ALL and NEL, were associated with shorter progression-free survival (PFS). From pre- to post-RT, there was a reduction in nCBV and nPH and an increase in apparent diffusion coefficient (ADC). Patients with lower nRF values at pre-RT, or a larger increase in nRF from pre-RT to post-RT, had significantly longer PFS. Time-dependent analysis showed that patterns of changes in ADC and anatomic volumes were associated with OS, while changes in nCBV, nPH, and the contrast-enhancing volume were associated with PFS. Our studies suggest that quantitative MRI variables derived from anatomic and physiological MRI provide useful information for predicting outcome in patients with GBM.

Keywords: magnetic resonance imaging, glioblastoma multiforme, survival.

Received June 23, 2010; accepted December 20, 2010.

Presented at the International Society for Magnetic Resonance in Medicine, Honolulu, April 18–24, 2009, and the 2010 annual meeting of the American Society of Clinical Oncology, Chicago, June 4–8.

Corresponding Author: Yan Li, UCSF Radiology Box 2532, Byers Hall, 1700 4th Street, San Francisco, CA 94158-2532 (yan.li@radiology.ucsf.edu.)

Gliomas account for the majority of primary brain tumors and vary from benign to malignant. Glioblastoma multiforme (GBM) represents the highest grade of glioma and is both the most common and the most malignant subtype. Treatment for patients with GBM includes maximal safe resection, radiation therapy (RT), and chemotherapy. The median survival that is reported in clinical trials is typically 15 months[1] but there is considerable variability among individuals, with some patients benefitting from more aggressive therapies. GBMs are highly infiltrative, and recurrence typically occurs in adjacent brain tissue within 2 cm of the original tumor site. Early assessment of prognosis, accurate grading, and determination of tumor burden and response to therapy are thus of great importance for all phases of treatment planning and patient care.

MRI is the standard imaging method in the evaluation of patients with brain tumors because it is able to delineate structural abnormalities. The standard

criteria for assessing tumor progression and response to therapy are based upon changes in cross-sectional diameters of the contrast-enhancing lesion (CEL) on post-gadolinium (Gd) T1-weighted images.[2] This represents the regions where the blood–brain barrier (BBB) has been compromised. The region of T2 hyperintensity is larger than the CEL but fails to distinguish between edema, gliosis, inflammation, cyst, and active tumor. Methods that have been proposed as candidates for improving the sensitivity and specificity for defining tumor are diffusion-weighted imaging (DWI), which reflects tumor cellularity as well as breakdown of normal tissue architecture, and perfusion-weighted imaging (PWI), which provides information on vascular density and abnormality.[3]

Previously published research revealed several factors—such as age, KPS score, extent of resection, molecular markers, presence of corticosteroid, and whether the patient undergoes reoperation at the time of recurrence—that influence the prognosis of patients with GBM.[4–11] Preoperative and preradiation MRI characteristics of the tumor have been reported as having predictive value in relation to survival.[12–14] Since not all the surgeries of patients enrolled in this study were completed in our institution and previous studies have noted the importance of assessment after surgery and prior to RT, we evaluated the relationship between serial MR parameters and overall survival (OS) and progression-free survival (PFS) in patients with primary GBM from this time point. We hypothesized that serial changes in imaging parameters would be helpful in anticipating disease progression and can be of prognostic value, which would be useful in making decisions about patient care.

Materials and Methods

Patient Population

All patients' charts were reviewed, and the GBM was called "primary" if there was no clinical or imaging history to suggest a lower grade tumor that progressed. A total of 66 patients with newly diagnosed primary GBM who were evaluated at the University of California–San Francisco after surgery and prior to initiation of RT were recruited to this imaging study. Each patient gave written informed consent to undergo the specialized imaging. Two patients were excluded from the analysis: one patient died of hepatitis B virus infection before progression, and the other had incomplete imaging data due to significant surgical complications. The remaining 64 patients constituted the study population.

Patients had their baseline scans after surgical resection or biopsy but prior to RT and chemotherapy (pre-RT), immediately after RT (post-RT) and every 2 months thereafter until presumed tumor progression (up to a maximum of 1 year). When tumor progression was suspected, patients received an additional scan at a short time interval (~1 month) to help in distinguishing true from pseudoprogression. Criteria for defining true progression were clinical deterioration and/or radiological progression, which was based upon changes in cross-sectional diameters of the CEL as defined by McDonald criteria,[2] or as confirmed by a second surgery. Pre-RT MR examinations were obtained following surgery or biopsy (mean $\pm$ standard deviation, 26 ± 8 days). Of the 57 patients for whom the exact start date of RT was recorded, pre-RT examinations were acquired at an average of 6 days (standard deviation, 6 days) before RT. RT was administered with a total dose of 60 Gy in 2-Gy fractions over a 6-week period. Chemotherapy was given concurrently either as temozolomide alone (23 patients), temozolomide with tarceva (29 patients), poly ICLC (10 patients), or R115777 (2 patients).

MR Examination

MR data were acquired from either 1.5 T or 3 T GE scanners (GE Healthcare Technologies) between November 2002 and March 2007.

Anatomic MR imaging included a T1-weighted sagittal scout (repetition time [TR]/echo time [TE] = 54/2 ms), axial T2-weighted fluid attenuated inversion recovery (FLAIR) (TR/TE/inversion time [TI] = 10002/127–157/2200 ms, matrix = 256 × 256 × 48, slice thickness = 3 mm), and pre- and postcontrast T1-weighted spoiled gradient echo (SPGR) (TR/TE = 26/2–8 ms, matrix = 256 × 256 × 64, slice thickness = 3 mm) images. These images were aligned to the corresponding post-Gd 3D SPGR images.[15]

Diffusion-weighted images were acquired with 3- or 6-directional axial diffusion echo-planar imaging (EPI) sequences (TR/TE = 5000–10000/63–110 ms, matrix = 128 × 128 or 256 × 256, slice thickness = 3–5 mm, 21–40 slices, b = 1000 s/mm^2). The ADC maps were calculated using software developed in our group, resampled to the same resolution as the postcontrast T1-weighted images, and then rigidly aligned to them using the VTK CISG software package.[16]

A bolus of 0.1 mmol/kg of body weight gadolinium diethyltriamine pentaacetic acid (Gd-DTPA) was injected intravenously at the speed of 5 mL/s. Perfusion-weighted images were achieved by collecting a series of T2*-weighted EPI (TR/TE/Flip = 1000–2000/54 ms/30–35°, 128 × 128 matrix, slice thickness = 3–5 mm, 7–15 slices, 60–80 timepoints) acquired before, during, and after the bolus injection. Perfusion datasets were resampled to the same resolution as the postcontrast T1-weighted images and then rigidly or nonrigidly aligned using the VTK CISG software package.[16] Cerebral blood volume (CBV), percent ΔR2* signal recovery (Rec), ΔR2* peak heights (PHs), and recirculation factors (RFs) were calculated for each voxel using software developed in our group. CBV intensities were obtained by fitting the dynamic perfusion data by a modified gamma-variate function with a recirculation parameter.[17] Peak height and percent recovery values were estimated using a simple nonparametric procedure.[18]

Image Analysis

Regions of interest (ROIs) included the normal-appearing white matter (NAWM), the CEL, the T2ALL, and the NEL, which was defined as the T2ALL lesion subtracted from the CEL and necrosis (Figure 1). NAWM was segmented automatically using a hidden Markov random field model with an expectation-maximization algorithm[19] on the 3D SPGR brain images. The masks of tumor lesions were segmented using a region-growing segmentation tool.[20] All ROIs excluded the resection cavity.

Volumetric, diffusion, and perfusion parameters were analyzed within these abnormalities. Due to smaller acquisition coverage of DWI and PWI compared with the anatomic images, these parameters were limited to the region that overlapped. To emphasize any difference between patients, ADC, CBV, PH, and RF maps were normalized to the median value within NAWM. The value of Rec is calculated as a percentage of the baseline and was therefore not normalized.

Statistics

The statistical analysis was performed using the SPSS software package and R version 2.9.2 (www.r-project.org). OS and PFS were estimated by using Kaplan–Meier survival curves. OS was determined from the date of the MR examination prior to RT and the date of death or last contact at which the patient was known to be alive (censored) as of January 31, 2009. PFS was defined as the time from the baseline scan to disease progression or death due to any cause, whichever came first. Since disease progression was tracked regularly for only up to one year, PFS was censored at the 1-year visit for those individuals who were alive and free of progression at that time. Survival curves for the various subgroups were compared using the log-rank test. One month was calculated as 30 ± 10 days.

A Cox proportional hazards model was used to evaluate the influences of pre-RT and post-RT MR parameters and the difference of MR variables between these two time points on OS and PFS. Patients who progressed at the time of post-RT were excluded from the post-RT analysis, and patients who were scanned at a different field strength at the time of post-RT than pre-RT were left out of the analysis when testing for significant difference between pre-RT and post-RT. A nonparametric Wilcoxon signed-rank test was used to access significance between time points. To evaluate the impact of change in imaging values over time on clinical outcome, we used a time-dependent Cox proportional hazards model treating the longitudinal image values as time-dependent covariates.[21] All the Cox model analyses were adjusted by age and field strength. Due to the exploratory nature of the study, no formal adjustment of type I error was undertaken; in all cases, a p-value <0.05 was considered statistically significant.

Results

Patient Characteristics and Outcomes

Table 1 summarizes the characteristics of the patient population, and Figure 2 shows the time to progression and status for each patient. It was noted that 73% of the patients (47/64) progressed within a year, as confirmed by follow-up imaging criteria (23/47) or by a second surgery (24/47). Of the 47 patients who progressed, 20 received a new type of chemotherapy alone (P-C), 24 had new therapy in combination with a second surgical resection (P-C + S), and data were not available for 3 patients. Sixteen patients progressed by the time of post-RT scan, with 10 of these assessments being confirmed by surgical resection. Of the patients who received a second surgery, histopathology of the resected tissue showed recurrent GBM.

The median OS was 588 days (95% CI, 468–708 days) with 11 patients censored, and the median PFS was 186 days (95% CI, 136–236 days) with 17 patients censored. Figure 3A and 3B illustrate the OS and PFS

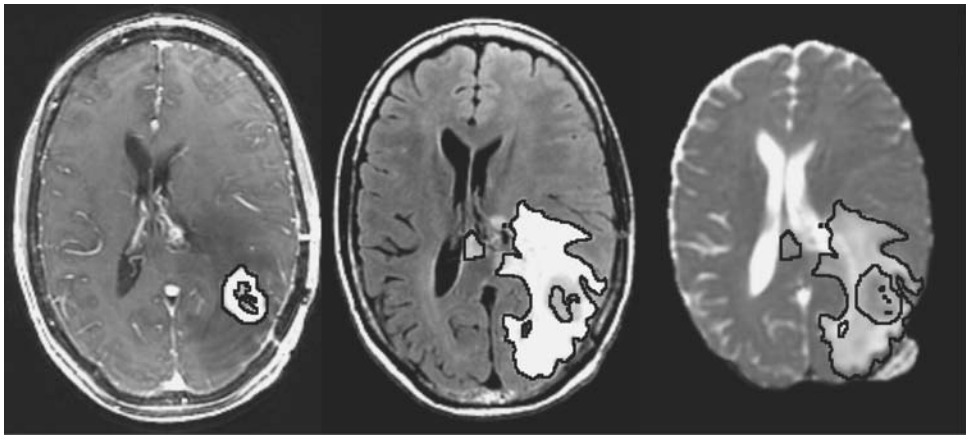

Fig. 1. Axial T1-weighted postcontrast, FLAIR, and ADC maps from a patient with GBM. Lines represent CEL, T2ALL, and NEL contours, respectively.

curves. In the univariate analysis, age, sex, KPS, steroids, extent of resection, and type of chemotherapy were not significantly correlated with OS or with PFS. Treatment failure or progression, by either 6 months or 12 months, was associated with a significant survival disadvantage (Fig. 3C-D, log-rank tests, $p = 0.0008$, $p < 0.0001$). In patients who progressed, the median survival times were 351 days and 619 days, respectively. This contrasted with 792 days or 1833 days in patients who were stable at 6 months or 12 months, respectively. There was no difference in survival between patients who had a PFS of less than 6 months and those who progressed between 6 and 12 months (Fig. 3E, log-rank test, $p = 0.80$), with patients who progressed by 6 months (PFS <6 mos) having a median survival time of 351 days (95% CI, 229–473), and patients who progressed between 6 months and 12 months (PFS 6–12 mos) surviving for 342 days (95% CI, 395–659). Patients who received a combination of reoperation and new chemotherapy (P-C + S) had significantly longer survival than those who received new chemotherapy alone (P-C) ($p < 0.0001$, log-rank test) (Fig. 3F). The median survival was 558 days (95% CI, 448–668 days) for the former and 342 days (95% CI, 105–579 days) for the latter. Only 2 of the patients who progressed received anti-angiogenic therapy at the time of recurrence.

Table 1. Baseline Characteristics of All Study Subjects

Characteristics	All Study Subjects
Age, yr	
Median	53
Range	27–77
Gender, n	
Male	38
Female	26
Karnofsky performance	
Median, %	90
Range, %	60–100
Data missing, n	16
Corticosteroid therapy, n	
Yes	36
No	21
Data missing	7
Extent of surgery, n	
Biopsy	3
Subtotal resection	29
Gross total resection	32

Imaging Characteristics

A total of 291 examinations were acquired from 64 patients (see Table 2). DWI data were acquired for 278 of the 291 examinations, and PWI data were available for 263 of the 291 examinations. The nonlinear fitting procedure for estimating CBV and RF was more demanding in terms of the data quality required to obtain stable parameter estimates, and so 241/263 of these datasets were used for the CBV/RF analysis,

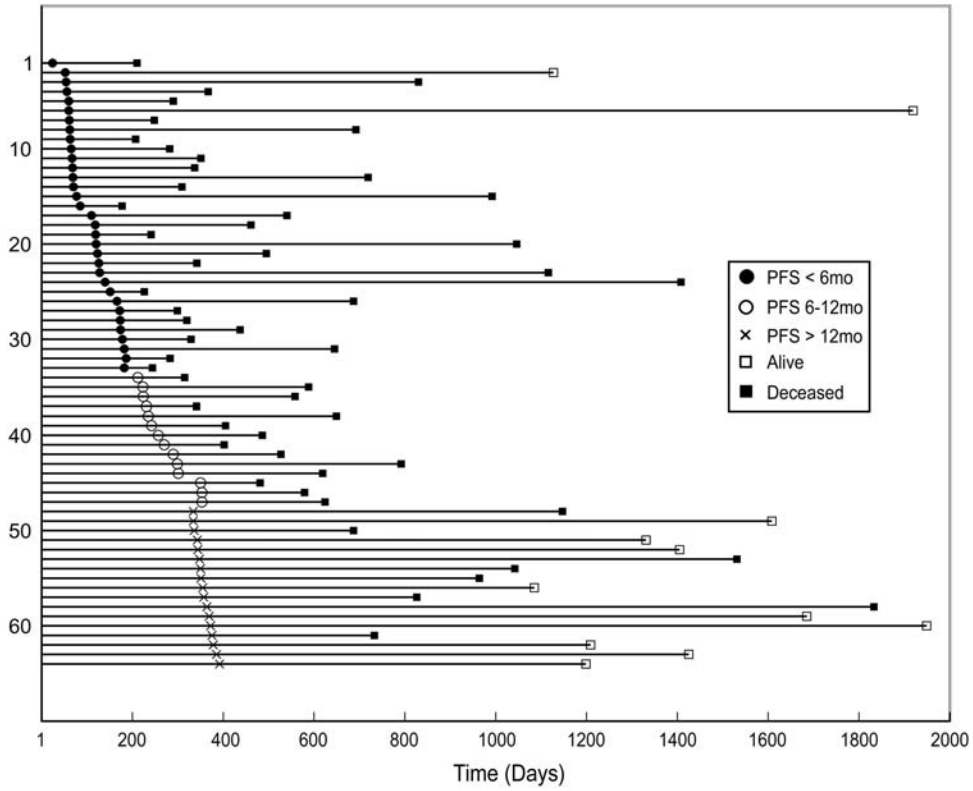

Fig. 2. Event chart for the 64 patients who were followed in the study. Each line represents a single patient. Patients are sorted by PFS.

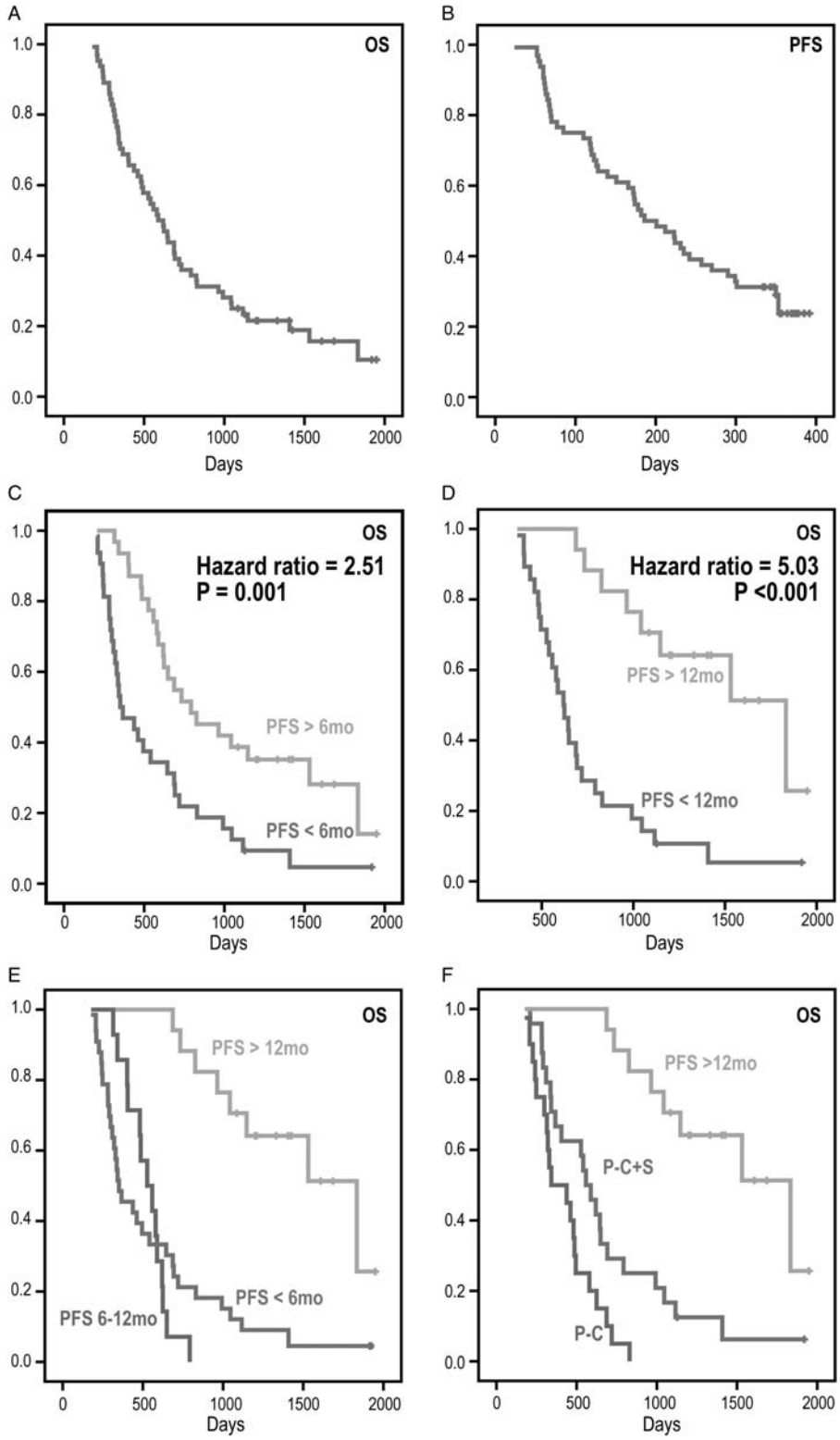

Fig. 3. Kaplan–Meier survival curves for OS and PFS. The median OS (A) was 588 days, and median PFS (B) was 186 days. Survival curves (C) and (D) are for populations split based upon whether the patient progressed or was stable by 6 months and 12 months. Patients who progressed within 6 months or 12 months had shorter survival; but there was no significant difference between patients who progressed by 6 months and patients who progressed between 6 and 12 months (E). Patients who progressed within a year benefited from the combination of reoperation and chemotherapy (P-C + S) (F).

Table 2. Number of Datasets for Each Imaging Parameter within the ROIs Considered

	CEL	T2ALL	NEL	NAWM
Vol	245	291	290*	291
ADC	233	278	278	278
CBV/RF	199	241	241	241
PH/Rec	214	260	260	260

*1 dataset was acquired without contrast injection.

while 260/263 of these datasets were considered for PH/Rec. Imaging parameters that were found to be significant predictors of OS and PFS at a significant level of 0.05 or lower based on the Cox regression model that was adjusting for age and field strength are summarized in Table 3.

Baseline Imaging Parameters

The only pre-RT imaging parameters that were related to OS were the volumes of the T2ALL and NEL. There was no association between any of these volumes and PFS. Table 4 shows the median and 10th/90th percentile values for nCBV, nPH, nRF, and %Rec in the anatomic ROIs. Note that all of the parameters considered including nCBV, nPH, and nRF were higher in the subpopulation who progressed by 12 months than in the subpopulation who did not, but only the values in the T2ALL and NEL were found to be significantly associated with PFS but not with OS. Figure 4 shows examples of anatomic images, nCBV and nPH maps from 2 patients at pre-RT. The patient who had regions with elevated nCBV and nPH in the T2ALL had relatively shorter PFS (128 days vs. stable at 378 days). None of the pre-RT diffusion parameters were associated with OS or PFS in this population.

Changes in Imaging Parameters between Pre-RT and Post-RT

Table 5 shows the normalized perfusion parameters at the time of pre-RT and post-RT. There were significant decreases in nCBV and nPH in all three anatomic ROIs from pre- to post-RT. The differences in the nRF and %Rec values were relatively small, and none of those changes was significant. Larger median nCBV in the T2ALL and NEL at post-RT was significantly associated with shorter PFS ($p = 0.026$ and 0.029). The differences between post-RT and pre-RT in 90th percentile nRF values within the T2ALL and NEL were significant factors for PFS. Patients with increased 90th nRF in T2ALL and NEL had a significant benefit in PFS (hazard ratio, 0.346, 0.339; $p = 0.046$, 0.037). In patients with PFS >12 mos, the mean $\pm$ standard deviation of 90th nRF in T2ALL and NEL was 0.98 ± 2.27 and 0.98 ± 2.28; in contrast, there were 0.00 ± 0.72 and 0.00 ± 0.69 in patients with PFS <12 mos, respectively.

Table 3. Significant ($p < 0.05$) Predictors of OS and PFS

	OS	PFS
Patient info	Response failure, 12 mos*** (5.031)	
	Response failure, 6 mos** (2.506)	
Pre-RT	Volume T2ALL (1.016)	Median nPH in T2ALL* (3.007)
	Volume NEL (1.017)	Median nCBV in T2ALL (2.414)
		Median nRF in NEL (8.352)
		Median nPH in NEL (2.481)
		Median nRF in T2ALL (7.101)
		Median nCBV in NEL (2.350)
Post-RT	Volume T2ALL* (1.010)	Median nCBV in T2ALL (5.180)
	Volume NEL* (1.011)	Median nCBV in NEL (5.029)
	Volume CEL* (1.042)	
[Post-pre]-RT		90th nRF in NEL (0.339)
		90th nRF in T2ALL (0.346)
Time-dependent	Volume T2ALL*** (1.013)	Median nCBV in T2ALL* (3.927)
	Volume NEL*** (1.014)	Median nPH in T2ALL (3.592)
	Volume CEL** (1.048)	Median nCBV in NEL (3.339)
	Median nADC in CEL* (0.143)	Volume CEL (1.036)
	10th nADC in NEL (21.708)	
	10th nADC in T2ALL (21.320)	
	10th nADC in CEL (0.123)	
	Median nADC in T2ALL (5.717)	
	Median nADC in NEL (4.727)	

All the tests were adjusted by age and field strength, and values are in the order of p-value from the smallest to the largest. Numbers in parentheses are hazard ratios.
*$p < 0.01$.
**$p < 0.001$.
***$p < 0.0001$.

The differences in normalized ADC (nADC) parameters in the various anatomic regions are shown in Table 6. The median and 10th percentile values of nADC were significantly larger in all anatomic regions after RT compared with the initial values, but none of the parameters was related to OS or PFS.

As shown in Table 3, the only parameters that were related to OS at the post-RT time points were the volumes of the three anatomic lesions (CEL, T2ALL, and NEL).

Table 4. Perfusion-Weighted Imaging Parameters, Normalized CBV (nCBV), Normalized Peak Height (nPH), Normalized Recirculation Factor (nRF), and Recovery (%Rec) at the Time of Pre-RT.

		PFS <12 mo	PFS >12 mo	HR (95% CI)	*p*-Value
Median nCBV	CEL	1.40 ± 0.79	1.26 ± 0.67		>0.05
	T2ALL	1.13 ± 0.45	0.92 ± 0.27	2.414 [1.147 5.082]	0.020
	NEL	1.06 ± 0.39	0.89 ± 0.27	2.350 [1.022 5.403]	0.044
90th nCBV	CEL	2.65 ± 1.41	2.36 ± 0.11		>0.05
	T2ALL	2.30 ± 1.09	1.95 ± 0.65		>0.05
	NEL	2.01 ± 0.75	1.76 ± 0.55		>0.05
Median nPH	CEL	1.49 ± 0.78	1.34 ± 0.63		>0.05
	T2ALL	1.13 ± 0.41	0.91 ± 0.26	3.007 [1.401 6.542]	0.005
	NEL	1.04 ± 0.37	0.88 ± 0.25	2.481 [1.112 5.533]	0.026
90th nPH	CEL	2.99 ± 1.53	2.55 ± 1.05		>0.05
	T2ALL	2.61 ± 1.26	2.14 ± 0.71	1.294 [0.998 1.678]	0.052
	NEL	2.27 ± 1.01	1.97 ± 0.60		>0.05
Median nRF	CEL	1.23 ± 0.36	1.20 ± 0.36		>0.05
	T2ALL	1.09 ± 0.14	0.98 ± 0.14	7.101 [1.090 46.281]	0.040
	NEL	1.08 ± 0.16	0.96 ± 0.12	8.352 [1.357 51.408]	0.022
90th nRF	CEL	2.14 ± 0.49	2.08 ± 0.57		>0.05
	T2ALL	1.77 ± 0.46	1.62 ± 0.38		>0.05
	NEL	1.68 ± 0.49	1.53 ± 0.30		>0.05
Median %Rec	CEL	92 ± 6	89 ± 15		>0.05
	T2ALL	96 ± 5	98 ± 5		>0.05
	NEL	97 ± 5	99 ± 4		>0.05
10th %Rec	CEL	68 ± 15	65 ± 21		>0.05
	T2ALL	79 ± 11	77 ± 18		>0.05
	NEL	81 ± 11	81 ± 13		>0.05

HR, hazard ratio; CI, confidence interval.

Time-dependent Analysis

Parameters that were significantly associated with PFS in the time-dependent analysis were the median nCBV in the T2ALL ($p = 0.006$) and NEL ($p = 0.0181$), the median nPH in the T2ALL ($p = 0.0147$), and the volume of the CEL ($p = 0.0376$). Figure 5 demonstrates the changes in the volumes of the CEL, T2ALL, and NEL in terms of time of OS and PFS. Some patients who progressed show an initial reduction in anatomic lesion volume, but, as can be expected, patients with an overall increase in the volumes of their abnormalities appear to have worse OS.

Figure 5 also shows the median nADC values in the various regions over time. Although it appears that the patients who live for over 2 years have stable changes in median ADC within the T2ALL and NEL regions between pre- and post-RT, the difference between post-RT and pre-RT was not a significant predictor for OS using Cox regression analysis. The time-dependent Cox regression model showed that smaller nADC values (median and 10th percentile) within the CEL ($p = 0.008$, 0.016) and higher nADC (median and 10th percentile) with the T2ALL ($p = 0.018$, 0.011) and NEL ($p = 0.027$ 0.011) were associated with poor OS.

Discussion

MRI is the principal method being used to evaluate response to therapy and tumor progression in patients with GBM. The current study examined the predictive values of an integrated anatomic and diffusion- and perfusion-weighted imaging examinations that were obtained postsurgery, pretreatment, and at posttreatment follow-ups to determine whether the information obtained could contribute to predicting PFS and OS.

The median OS for the patients in this study with GBM was 84 weeks, but as seen from Figure 2, there is a large range of outcome values observed. Previous studies have found several variables that are associated with worse survival, but it is not known how these relate to each other.[4–11] Age did not reach significance in the population considered in this study but was adjusted for in the statistical analysis because it has previously been shown to act as a prognostic factor in studies with larger patient populations.[4,7,11] Extent of resection was also tested but was not found to be a significant factor. The importance of the extent of resection is still controversia1[7,11,22] and may influence decisions about the treatment that is chosen.[10] Other factors—such as tumor size, edema, midline shift, and location—that may affect resection and influence survival were not examined here due to the limited size of the population.

Disease progression was determined in this study based upon the size of the CEL in conjunction with neurologic function and corticosteroid use.[2] Patients who progressed by 6 months or 12 months had significantly shorter median survival time than those who did not. Although there was no difference in survival between patients who progressed by 6 months and

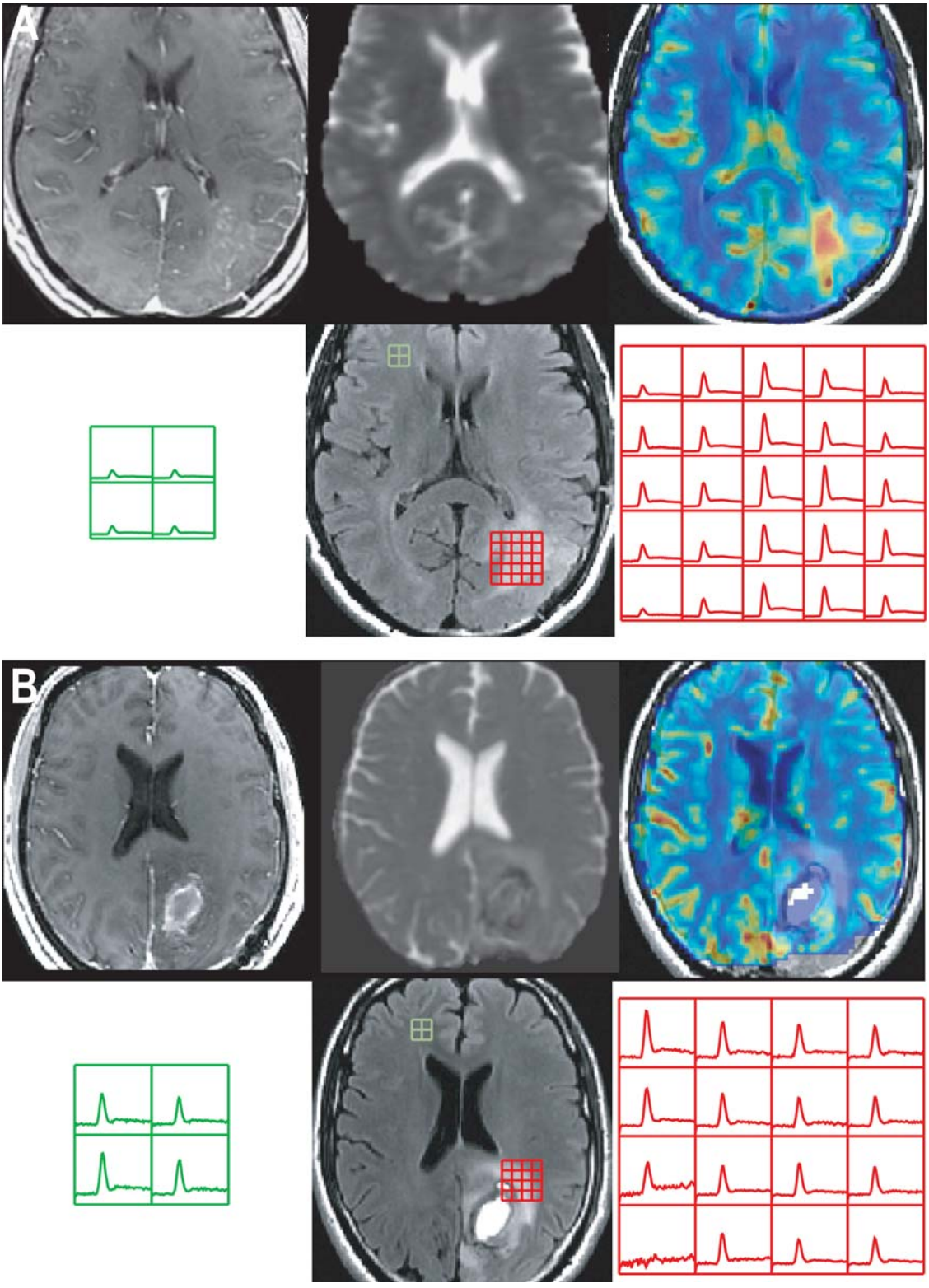

Fig. 4. Postcontrast T1-weighted, T2-weighted, ADC, nCBV, and nPH images from 2 patients with GBM and the corresponding ΔR2* curves showing the magnitude of PH and Rec parameters in the T2ALL and NAWM regions at pre-RT. All the nCBV and nPH maps were plotted with the range between 0 and 5. Patient A had a short PFS of 128 days, and Patient B was stable at 378 days.

12 months, the second-line therapies that they were given did influence OS, with the median survival of patients who received reoperation and other chemotherapy being significantly longer than that of patients who received chemotherapy alone. Reoperation in combination with other salvage therapy

Table 5. Median Values for Normalized Perfusion Parameters within Different Anatomic Regions at the Time of Pre-RT and Post-RT Time Points

		CEL	T2ALL	NEL
Median nCBV	Pre-RT	1.44 ± 0.87	1.04 ± 0.45	0.97 ± 0.39
	Post-RT	0.95 ± 0.47	0.88 ± 0.37	0.88 ± 0.37
		$N = 29$	$N = 33$	$N = 33$
		$p = 0.0005$	**$p = 0.001$**	**$p = 0.012$**
Median nPH	Pre-RT	1.45 ± 0.85	1.02 ± 0.37	0.96 ± 0.34
	Post-RT	1.09 ± 0.50	0.85 ± 0.32	0.84 ± 0.31
		$N = 33$	$N = 37$	$N = 37$
		$p = 0.010$	**$p = 0.001$**	**$p = 0.005$**
Median nRF	Pre-RT	1.26 ± 0.30	1.03 ± 0.15	1.01 ± 0.15
	Post-RT	1.26 ± 0.49	1.04 ± 0.48	1.03 ± 0.38
		$N = 29$	$N = 33$	$N = 33$
		$p > 0.05$	$p > 0.05$	$p > 0.05$
Median %Rec	Pre-RT	76 ± 10	80 ± 11	81 ± 10
	Post-RT	74 ± 14	82 ± 11	82 ± 11
		$N = 33$	$N = 37$	$N = 37$
		$p > 0.05$	$p > 0.05$	$p > 0.05$

Table 6. Median and 10th Percentile Intensity Values for Normalized ADC within Different Anatomic Regions at the Time of Pre-RT and Post-RT.

		CEL ($N = 37$)	T2ALL ($N = 40$)	NEL ($N = 40$)
Median nADC	Pre-RT	1.45 ± 0.39	1.38 ± 0.28	1.37 ± 0.27
	Post-RT	1.71 ± 0.34	1.49 ± 0.27	1.47 ± 0.27
		$p = 0.001$	$p = 0.015$	$p = 0.016$
10th nADC	Pre-RT	1.10 ± 0.28	1.06 ± 0.18	1.06 ± 0.18
	Post-RT	1.28 ± 0.25	1.17 ± 0.16	1.16 ± 0.15
		$p = 0.001$	$p = 0.0004$	$p = 0.0003$

has been reported to show a significantly prolonged survival compared with reoperation alone,[23] but the criteria for reoperation are still not standardized across institutions.[24,25]

Another interesting finding from our analysis was that the pre-RT contrast-enhancing volume was not related to OS. We believe that this is due to some areas of enhancing being postsurgical effects rather than tumor. Previous studies at our institution have indicated that areas showing restricted diffusion on the immediate postsurgical scan may become enhancing in follow-up scans.[26] When corrected for this effect, we have shown that an increase in the true volume of contrast enhancement between surgery and pre-RT is associated with shorter survival.[27] It was not possible to make an assessment of whether variations in the pre-RT enhancing lesion volume were due to this effect in the current study because not all of the patients considered received their surgery at our institution. The robustness of the relationship between the T2ALL and NEL volumes and OS observed in our study is enhancing and supports the idea that they may be used to assess the presence of residual disease.

Recent studies have shown that some patients with GBM suffer from a temporary increase in the CEL that subsides afterward without further treatment.[28,29] This effect has been termed pseudoprogression, and it commonly develops within 2 to 6 months after completion of concomitant RT plus temozolomide. Of the 47 patients who progressed during our study, 51% were confirmed as having true progression by the reoperation. For patients who did not get a resection, the assessment was based upon clinical and imaging follow-up, which included a repeat MR scan at 1-month intervals to assess whether the new enhancement was persistent. This strategy was intended to minimize any confounding effects caused by pseudoprogression.

Of interest in terms of determining which time point to consider in predicting outcome is that the volumes of all 3 anatomic lesions at the post-RT examination were related to OS. As shown in Figure 5, patients with worse survival had a larger volume of T2 hyperintensity after surgical resection at any given time point, even though none of the volumetric parameters were associated with PFS. The latter is not that surprising because some of the patients who progress show an initial reduction in lesion volume, and the definition of progression is based upon the change of contrast enhancement between the current and previous scans.

The observed decline in nCBV and nPH that we observed following radiation suggested that there was a reduction in vascular density due to the effects of RT and concurrent chemotherapy. The presence of regions with elevated nCBV and nPH at pre-RT and post-RT time points, as well as time-dependent changes in these values in all anatomic lesions, was correlated with shorter PFS. This is consistent with previous observations.[30, 31] As gliomas grow, their cellularity tends to increase, which may cause regional hypoxia due to inadequate vascular supply. Upregulation of vasoactive endothelial growth factor (VEGF) promotes the formation of new blood vessels by the process of angiogenesis.[32–35] The results of this study indicate that PWI can be used to monitor these effects. The fact that these parameters are not related to OS is not surprising given that there was so much change in them after a patient progressed. It also suggests that the relationship between tumor growth and abnormal angiogenesis in GBM is more complex than has previously been appreciated.

The recirculation and recovery parameters estimated from PWI data reflect increased vascular permeability and vessel tortuosity. Our results show that the presence of higher values of the recirculation parameter in the T2ALL and NEL at the pre-RT examination is associated with shorter PFS. In other words, patients who had more leaky vessels were more initially likely to progress at an early time point. Patients with smaller changes in the recirculation parameters between pre-RT and post-RT were more likely to show early

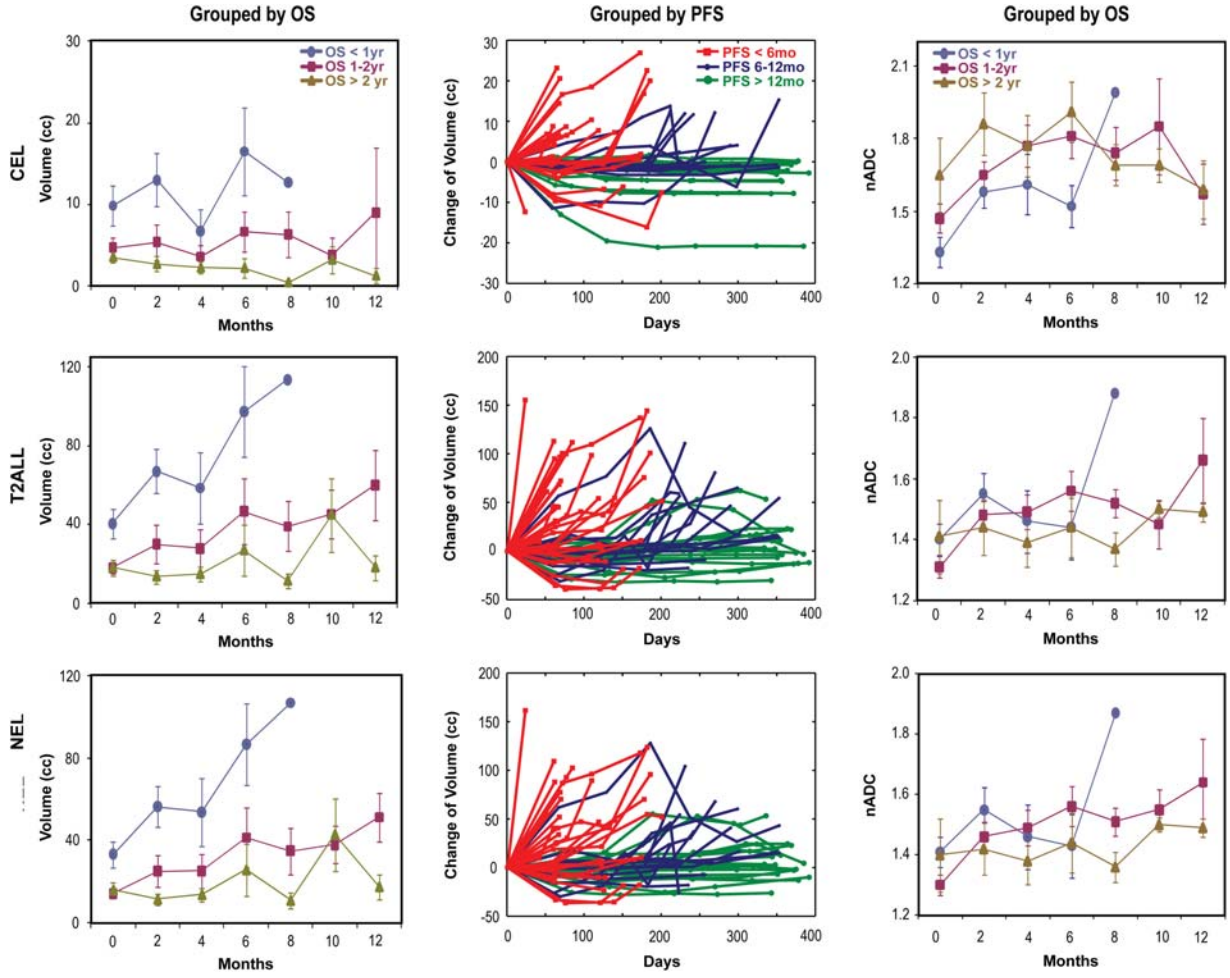

Fig. 5. [**Left**] The mean and standard deviation of the mean for volumes of abnormalities in each individual group over time. Higher volumes at any given time point are seen in patients who had shorter survival. The median volumes of the T2ALL in the patients who died within a year were 21.6 ($n = 19$), 53.6 ($n = 16$), 48.2 ($n = 8$), 104.3 ($n = 7$), and 113.6 cc ($n = 1$) at 0, 2, 4, 6, and 8 months, respectively, while they were 12.4 ($n = 13$), 9.6 ($n = 12$), 10.3 ($n = 10$), 10.1 ($n = 7$), 11.7 ($n = 4$), 30.6 ($n = 5$), and 11.8 cc ($n = 5$) at 0, 2, 4, 6, 8, 10, and 12 months in the population who lived longer than 2 years. [**Middle**] Changes in volume for patients with progression by 6 months (red), between 6 and 12 months (blue), and after 12 months (green). Note that some patients who progressed show an initial reduction in lesion volume. [**Right**] Time course of median nADC in 3 groups of GBM patients. Values refer to mean and standard deviation of the mean. Smaller nADC values in CEL and higher in T2ALL and NEL are seen in patients who died within a year.

progression. This suggests that the increased vascular permeability caused by RT[36,37] may facilitate more effective delivery of the chemotherapy through the BBB and hence provide time to prolong progression.

Low ADC within regions of tumor is thought to correspond to regions of higher cellularity, while increased ADC corresponds to edema or treatment effects.[38–40] In practice, both of these findings are present and may therefore counteract each other, especially once the lesion has been treated. Our data showed that there was a significant increase in nADC within all anatomic lesions after RT, which is consistent with the radiation causing increased disruption of tissue architecture and a decrease in cellularity that is associated with treatment-induced necrosis.[41] Unlike the change in vascular parameters, these structural and cell-based measures of treatment effect were not related to PFS but were associated with OS when looked at longitudinally in a time-dependent analysis. The differences in relationship to clinical outcome highlight the complexity of the processes associated with disease progression and treatment effects.

Although the normalized ADC values observed at pre-RT and post-RT were not significant prognostic factors, the time-dependent values were significantly correlated with OS. Interestingly, lower nADC in the CEL and higher nADC in the T2ALL and NEL were associated with worse survival in the time-dependent analysis. This may be interpreted as the ADC in the enhancing volume being dominated by increased tumor cellularity, with the changes in ADC in the nonenhancing volume being associated with infiltrative tumor causing a breakdown of the normal tissue architecture. The potential for uncoupling these effects is interesting but highlights the

complexity of interpreting changes in ADC. It is for this reason that the function diffusion map has been proposed as a measure of the sum of positive and negative changes in ADC on a pixel-by-pixel basis within the enhancing region as opposed to more global parameters. Our study suggests that it may be of interest to separately examine the temporal changes in enhancing and nonenhancing volumes separately.

The relatively short median survival for GBM patients has led to the development of therapeutic agents that are designed to act either by inhibiting angiogenesis or blocking cell proliferation.[42–44] Anti-angiogenic or antiproliferative therapies that suppress tumor growth, rather than directly causing cell death may cause reduction in the incidence of CELs without a concurrent decrease in the number of tumor cells. This means that increases in the spatial extent of the T2 hyperintense lesions will be critical for assessing recurrence.[45] Even in our study, where the majority of patients (81%) received only temozolomide and radiation, the volume of the T2ALL was related to OS. Future studies will use similar multiparametric anatomic and diffusion- and perfusion-weighted imaging methods to follow patients participating in clinical trials using novel treatment strategies.

Conclusion

Our study has highlighted differences in the temporal and spatial patterns of MR parameters derived from anatomic and diffusion- and perfusion-weighted images from patients with newly diagnosed primary GBM being treated with radiation and concurrent chemotherapy. At the pretreatment time point, we found that higher blood volumes, peak height, and recirculation factors in the T2 lesion were associated with PFS, while nonenhancing and T2 lesion volumes were associated with OS. By the end of radiation, there was a reduction in blood volume and peak height, with an increase in the observed ADC values within all anatomic regions. This is consistent with reduced vascular density and the formation of treatment-induced necrosis. Time-dependent analysis showed that patterns of changes in ADC and anatomic volumes were associated with OS, while changes in blood volume, peak height, and enhancing volume were associated with PFS. This indicates that a multiparametric MR examination that integrates anatomic and perfusion- and diffusion-weighted imaging can provide useful information for predicting outcome and understanding treatment effects in patients with GBM.

Conflict of interest statement. None declared.

Acknowledgments

The authors thank Michael C. Lee, Gabriela Bourne, and Collen McGue for their assistance with data collection and analysis, as well as helpful comments regarding this manuscript.

Funding

This study was supported by UC Discovery grant ITL-BIO04-10148; NIH grants R01 CA127612 and NIH P50 CA97257; and a grant from the Joelle Syverson American Brain Tumor Association Fellowship.

References

1. Stupp R, Mason WP, van den Bent MJ, et al. Radiotherapy plus concomitant and adjuvant temozolomide for glioblastoma. *N Engl J Med.* 2005; 352:987–996.
2. Macdonald DR, Cascino TL, Schold SC, Jr., Cairncross JG. Response criteria for phase II studies of supratentorial malignant glioma. *J Clin Oncol.* 1990; 8:1277–1280.
3. Yang I, Aghi MK. New advances that enable identification of glioblastoma recurrence. *Nat Rev Clin Oncol.* 2009; 6:648–657.
4. Burger PC, Green SB. Patient age, histologic features, and length of survival in patients with glioblastoma multiforme. *Cancer.* 1987; 59:1617–1625.
5. Hohwieler Schloss M, Freidberg SR, Heatley GJ, Lo TC. Glucocorticoid dependency as a prognostic factor in radiotherapy for cerebral gliomas. *Acta Oncol.* 1989; 28:51–55.
6. Etienne MC, Formento JL, Lebrun-Frenay C, et al. Epidermal growth factor receptor and labeling index are independent prognostic factors in glial tumor outcome. *Clin Cancer Res.* 1998; 4:2383–2390.
7. Lacroix M, Abi-Said D, Fourney DR, et al. A multivariate analysis of 416 patients with glioblastoma multiforme: prognosis, extent of resection, and survival. *J Neurosurg.* 2001; 95:190–198.
8. Hegi ME, Diserens AC, Gorlia T, et al. MGMT gene silencing and benefit from temozolomide in glioblastoma. *N Engl J Med.* 2005; 352:997–1003.
9. Stark AM, Hedderich J, Held-Feindt J, Mehdorn HM. Glioblastoma—the consequences of advanced patient age on treatment, survival. *Neurosurg Rev.* 2007; 30:56–61; discussion 61–62.
10. Stummer W, Reulen HJ, Meinel T, et al. Extent of resection and survival in glioblastoma multiforme: identification of and adjustment for bias. *Neurosurgery.* 2008; 62:564–576; discussion 564–576.
11. Filippini G, Falcone C, Boiardi A, et al. Prognostic factors for survival in 676 consecutive patients with newly diagnosed primary glioblastoma. *Neuro Oncol.* 2008; 10:79–87.
12. Hammoud MA, Sawaya R, Shi W, Thall PF, Leeds NE. Prognostic significance of preoperative MRI scans in glioblastoma multiforme. *J Neurooncol.* 1996; 27:65–73.
13. Saraswathy S, Crawford FW, Lamborn KR, et al. Evaluation of MR markers that predict survival in patients with newly diagnosed GBM prior to adjuvant therapy. *J Neurooncol.* 2009; 91:69–81.
14. Crawford FW, Khayal IS, McGue C, et al. Relationship of pre-surgery metabolic and physiological MR imaging parameters to survival for patients with untreated GBM. *J Neurooncol.* 2009; 91:337–351.

15. Nelson SJ, Nalbandian AB, Proctor E, Vigneron DB. Registration of images from sequential MR studies of the brain. *J Magn Reson Imaging.* 1994; 4:877–883.
16. Hartkens T, D. R, Schnabel JA, Hawkes DJ, Hill DLG. VTK CISG Registration Toolkit: An open source software package for affine and non-rigid registration of single- and multimodal 3D images. In: BVM; 2002; Leipzig, Germany: Springer-Verlag, 2002: Abstract 185.
17. Lee MC, Cha S, Chang SM, Nelson SJ. Dynamic susceptibility contrast perfusion imaging of radiation effects in normal-appearing brain tissue: changes in the first-pass and recirculation phases. *J Magn Reson Imaging.* 2005; 21:683–693.
18. Lupo JM, Cha S, Chang SM, Nelson SJ. Dynamic susceptibility-weighted perfusion imaging of high-grade gliomas: characterization of spatial heterogeneity. *AJNR Am J Neuroradiol.* 2005; 26:1446–1454.
19. Zhang Y, Brady M, Smith S. Segmentation of brain MR images through a hidden Markov random field model and the expectation-maximization algorithm. *IEEE Trans Med Imaging.* 2001; 20: 45–57.
20. Saraswathy S, Crawford F, Nelson SJ. Semi-automated segmentation of brain tumor lesions in MR images. In: *14th Annual Meeting of ISMRM*; 2006; Abstract 1609.
21. Aydemir U, Aydemir S, Dirschedl P. Analysis of time-dependent covariates in failure time data. *Stat Med.* 1999; 18:2123–2134.
22. Kreth FW, Berlis A, Spiropoulou V, et al. The role of tumor resection in the treatment of glioblastoma multiforme in adults. *Cancer.* 1999; 86:2117–2123.
23. Mandl ES, Dirven CM, Buis DR, Postma TJ, Vandertop WP. Repeated surgery for glioblastoma multiforme: only in combination with other salvage therapy. *Surg Neurol.* 2008; 69:506–509; discussion 509.
24. Soults CB, Canute GS, Ryken TC. Evidence-based review of the role of reoperation in the management of malignant glioma. *Neurosurg Focus.* 1998; 4:e11.
25. Barbagallo GM, Jenkinson MD, Brodbelt AR. 'Recurrent' glioblastoma multiforme, when should we reoperate? *Br J Neurosurg.* 2008; 22:452–455.
26. Smith JS, Cha S, Mayo MC, et al. Serial diffusion-weighted magnetic resonance imaging in cases of glioma: distinguishing tumor recurrence from postresection injury. *J Neurosurg.* 2005; 103:428–438.
27. Pirzkall A, McGue C, Saraswathy S, et al. Tumor regrowth between surgery and initiation of adjuvant therapy in patients with newly diagnosed glioblastoma. *Neuro Oncol.* 2009; 11:842–852.
28. Brandsma D, Stalpers L, Taal W, Sminia P, van den Bent MJ. Clinical features, mechanisms, and management of pseudoprogression in malignant gliomas. *Lancet Oncol.* 2008; 9:453–461.
29. Chaskis C, Neyns B, Michotte A, De Ridder M, Everaert H. Pseudoprogression after radiotherapy with concurrent temozolomide for high-grade glioma: clinical observations and working recommendations. *Surg Neurol.* 2009; 72:423–428.
30. Cha S, Knopp EA, Johnson G, et al. Dynamic contrast-enhanced T2-weighted MR imaging of recurrent malignant gliomas treated with thalidomide and carboplatin. *AJNR Am J Neuroradiol.* 2000; 21:881–890.
31. Bisdas S, Kirkpatrick M, Giglio P, Welsh C, Spampinato MV, Rumboldt Z. Cerebral blood volume measurements by perfusion-weighted MR imaging in gliomas: ready for prime time in predicting short-term outcome and recurrent disease? *AJNR Am J Neuroradiol.* 2009; 30:681–688.
32. Wesseling P, Ruiter DJ, Burger PC. Angiogenesis in brain tumors; pathobiological and clinical aspects. *J Neurooncol.* 1997; 32:253–265.
33. Damert A, Machein M, Breier G, et al. Up-regulation of vascular endothelial growth factor expression in a rat glioma is conferred by two distinct hypoxia-driven mechanisms. *Cancer Res.* 1997; 57: 3860–3864.
34. Amoroso A, Del Porto F, Di Monaco C, Manfredini P, Afeltra A. Vascular endothelial growth factor: a key mediator of neoangiogenesis. A review. *Eur Rev Med Pharmacol Sci.* 1997; 1:17–25.
35. Brat DJ, Van Meir EG. Glomeruloid microvascular proliferation orchestrated by VPF/VEGF: a new world of angiogenesis research. *Am J Pathol.* 2001; 158:789–796.
36. Trnovec T, Kallay Z, Bezek S. Effects of ionizing radiation on the blood brain barrier permeability to pharmacologically active substances. *Int J Radiat Oncol Biol Phys.* 1990; 19:1581–1587.
37. Rubin P, Gash DM, Hansen JT, Nelson DF, Williams JP. Disruption of the blood-brain barrier as the primary effect of CNS irradiation. *Radiother Oncol.* 1994; 31:51–60.
38. Kono K, Inoue Y, Nakayama K, et al. The role of diffusion-weighted imaging in patients with brain tumors. *AJNR Am J Neuroradiol.* 2001; 22:1081–1088.
39. Guo AC, Cummings TJ, Dash RC, Provenzale JM. Lymphomas and high-grade astrocytomas: comparison of water diffusibility and histologic characteristics. *Radiology.* 2002; 224:177–183.
40. Muti M, Aprile I, Principi M, et al. Study on the variations of the apparent diffusion coefficient in areas of solid tumor in high grade gliomas. *Magn Reson Imaging.* 2002; 20:635–641.
41. Plowman PN. Stereotactic radiosurgery. VIII. The classification of post-radiation reactions. *Br J Neurosurg.* 1999; 13:256–264.
42. Lund EL, Spang-Thomsen M, Skovgaard-Poulsen H, Kristjansen PE. Tumor angiogenesis—a new therapeutic target in gliomas. *Acta Neurol Scand.* 1998; 97:52–62.
43. Franceschi E, Tosoni A, Bartolini S, Mazzocchi V, Fioravanti A, Brandes AA. Treatment options for recurrent glioblastoma: pitfalls and future trends. *Expert Rev Anticancer Ther.* 2009; 9:613–619.
44. Hsu JY, Wakelee HA. Monoclonal antibodies targeting vascular endothelial growth factor: current status and future challenges in cancer therapy. *BioDrugs.* 2009; 23:289–304.
45. van den Bent MJ, Vogelbaum MA, Wen PY, Macdonald DR, Chang SM. End point assessment in gliomas: novel treatments limit usefulness of classical Macdonald's Criteria. *J Clin Oncol.* 2009; 27: 2905–2908.